Low-Temperature Hydrothermal Deposition of $(Ba_xSr_{1-x})TiO_3$ Thin Films on Flexible Polymeric Substrates for Embedded Applications

Ru Z. Hou, Aiying Wu, and Paula M. Vilarinho*

Department of Ceramics and Glass Engineering, CICECO, University of Aveiro, 3810-193 Aveiro, Portugal

Received July 22, 2008. Revised Manuscript Received December 22, 2008

The fabrication of ferroelectric thin films on flexible metal foils or polymeric substrates is of particular interest for embedded capacitors integrated into Printed Circuit Boards (PCB). In this work, $Ba_xSr_{1-x}TiO_3$ ($x = 1$, 0.9, 0.7, 05, 0.3, 0.1, and 0) polycrystalline thin films were fabricated at low temperature (120 °C) and for a short time (1 h) by a hydrothermal process on commercial flexible polymeric Kapton films. Microstructural analysis showed that dense $BaTiO_3$ thin films comparable to those derived from long time hydrothermal processes were achieved with the present synthesis conditions. With increasing strontium content, $Ba_xSr_{1-x}TiO_3$ film thickness decreased and grain size increased. For $x = 0$, i.e., $SrTiO_3$, the films displayed a monolayer of coarse grains. The variation of the film morphology with the composition suggests a faster nucleation and reaction kinetics for $BaTiO_3$ than $SrTiO_3$. Electrical characterization showed high capacitance densities and acceptable dielectric loss for the films after postannealing in oxygen. Existence of polar domains in the hydrothermally synthesized $BaTiO_3$ thin films was proved by piezoresponse force microscopy (PFM). All the used processes were compatible with commercial Kapton films, showing the technological value of this work for the deposition of large area capacitors onto flexible printed circuits.

Introduction

The fast development of electronic industry is demanding Printed Circuit Boards (PCB) with embedded components when the density of current discrete components soldered on the surface of PCB is reaching the limit. Embedding capacitors into their packaging substrate has many benefits such as higher packaging density, lower parasitic effects, decrease in solder points, increase in device reliability, and improved signal integrity.[1] The use of various dielectric materials is of current interest for embedded capacitors: either pure or ceramic filled polymers, paraelectrics (Ta_2O_5, TiO_2), and ferroelectrics ($BaTiO_3$, $(Ba,Sr)TiO_3$, $Pb(Zr,Ti)O_3$), among which the well-known solid solution $(Ba_xSr_{1-x})TiO_3$ is very attractive due to their high dielectric constant, tunability of the dielectric constant with the electric field, possibility to tailor the properties via compositional modification, and the nontoxic lead free nature.

High-quality $(Ba_xSr_{1-x})TiO_3$ thin films can be prepared by magnetron sputtering, MOCVD, PLD, and Sol−Gel processes.[2−6] However, high deposition or heat treatment temperatures (usually >650 °C) are required to get crystalline films with desirable dielectric properties, which are unfortunately incompatible with any organic PCB substrate. A drastic reduction of the synthesis temperature of these ferroelectric materials is essential.

Hydrothermal process is a well-studied and widely accepted clean chemistry method for low temperature synthesis of various materials. There are numerous reports about hydrothermally prepared $BaTiO_3$ or $SrTiO_3$, either in the form of fine powders,[7−10] or thin films deposited on Ti-containing sol−gel amorphous precursor layers[11−13] or on Ti metal substrates.[14−18] Hydrothermal synthesis can be suitable and promising for embedding ferroelectric capacitors into PCBs due to its compatibility with some polymers and the feasibility of being scaled up. Low-temperature hydrothermal preparation and dielectric characterization of $BaTiO_3$ thin films on rigid epoxy PCB substrates were recently reported.[19,20]

* Corresponding author. Fax: 351 234 370204. E-mail: paula.vilarinho@ua.pt.

(1) Jillek, W.; Yung, W. K. C. *Int. J. Adv. Manuf. Technol.* **2005**, *25*, 350.
(2) Ezhilvalavan, S.; Tseng, T. Y. *Mater. Chem. Phys.* **2000**, *65*, 227.
(3) Ihlefeld, J. F.; Borland, W. J.; Maria, J. P. *Adv. Funct. Mater.* **2007**, *17*, 1199.
(4) Zhu, X.; Zhu, J.; Zhou, S.; Liu, Z.; Ming, N.; Lu, S.; Chan, H. L.-W.; Choy, C.-L. *J. Electron. Mater.* **2003**, *32*, 1125.
(5) Ianculescu, A.; Despax, B.; Bley, V.; Lebey, T.; Gavrila, R.; Dragan, N. *J. Eur. Ceram. Soc.* **2007**, *27*, 1129.
(6) Yuan, Z.; Lin, Y.; Weaver, J.; Chen, X.; Chen, C. L.; Subramanyam, G.; Jiang, J. C. *Appl. Phys. Lett.* **2005**, *87*, 152901.
(7) Dutta, P. K.; Gregg, J. R. *Chem. Mater.* **1992**, *4*, 843.
(8) Dutta, P. K.; Asiaie, R.; Akbar, S. A.; Zhu, W. *Chem. Mater.* **1994**, *6*, 1542.
(9) Feng, Q.; Hirasawa, M.; Yanagisawa, K. *Chem. Mater.* **2001**, *13*, 290.
(10) Moon, J.; Suvaci, E.; Morrone, A.; Costantino, S. A.; Adair, J. H. *J. Eur. Ceram. Soc.* **2003**, *23*, 2153.
(11) McCormick, M. A.; Slamovich, E. B. *J. Eur. Ceram. Soc.* **2003**, *23*, 2143.
(12) Xu, J.; Zhai, J.; Yao, X. *Appl. Phys. Lett.* **2006**, *89*, 252902.
(13) Wu, Z.; Kumagai, N.; Yoshimura, M. *Chem. Mater.* **2000**, *12*, 3356.
(14) Zhu, W.; Akbar, S. A.; Asiaie, R.; Dutta, P. K. *J. Electroceram.* **1998**, *2*, 21.
(15) Kajiyoshi, K.; Yanagisawa, K. *J. Phys.: Condens. Matter.* **2004**, *16*, S1351.
(16) Ishizawa, N.; Banno, H.; Hayashi, M.; Yoo, S. E.; Yoshimura, M. *Jpn. J. Appl. Phys.* **1990**, *29*, 2467.
(17) Kajiyoshi, K.; Yoshimura, M.; Hamaji, Y.; Tomono, K.; Kasanami, T. *J. Mater. Res.* **1996**, *11*, 169.
(18) Kajiyoshi, K.; Sakabe, Y.; Yoshimura, M. *Jpn. J. Appl. Phys.* **1997**, *36*, 1209.

10.1021/cm802845s CCC: $40.75
Published on Web 03/12/2009

The films prepared at the higher temperatures had a better quality with the reaction temperature varying from 80 to 200 °C. In both the reports, a long reaction time of 24 h was adopted. These works clearly indicate that such in situ material synthesis may provide a new technique to embed large area capacitors into organic substrate via a solution-based process. It is necessary to further investigate the polymer-compatible hydrothermal synthesis beyond these two existing reports, and expand to other materials, namely the $(Ba_xSr_{1-x})TiO_3$ solid solution. In addition, it is worth exploring the replacement of rigid PCB with flexible polymeric substrates, which enables flexibility of the circuit and leads to more space saving and weight reduction of the final devices. The first described case, in which flexible substrates were used in conjunction with hydrothermal synthesis, was reported for the synthesis of $BaTiO_3$ and $SrTiO_3$ thin films on polyphenylen sulfide sheet.[16] The replacement of rigid PCB, may bring more strict requirements to the hydrothermal synthesis conditions to avoid degradation of the flexible substrate in a highly alkaline solution. Thus, low hydrothermal temperature and short reaction time are desirable. Although hydrothermal synthesis at temperatures lower than 100 °C has been reported in the literature, seldom are there reports about the hydrothermal synthesis of $(Ba_xSr_{1-x})TiO_3$ with short processing time. Moreover, while detailed studies about the hydrothermal preparation of $(Ba_xSr_{1-x})TiO_3$ powders are well-known,[21−23] the knowledge on the equivalent synthesis of thin $(Ba_xSr_{1-x})TiO_3$ films is still insufficient.[24,25] The relations between composition and reaction kinetics of hydrothermal $(Ba_xSr_{1-x})TiO_3$ powders has been established, showing a higher reaction rate and faster particle growth as the barium content increases.[23] For films, the fact that the hydrothermal reaction and grain growth only occur on the surface of the substrate gives a spatial limitation which may affect the product morphology and the kinetics of the reaction compared with the powders, especially in the case of short hydrothermal reaction time compatible with polymeric flexible substrates. The clarification of this aspect was another motivation behind the present study.

Noticing that the reported works about hydrothermally prepared ferroelectric films were mainly focused on $BaTiO_3$ using rigid PCB substrates, in this work the preparation and characterization of $Ba_xSr_{1-x}TiO_3$ thin films on commercial flexible polymeric substrate "Kapton" via a short-time hydrothermal process is aimed. Katpon (Kapton polyimide film) developed by DuPont is a durable film which remains stable in the temperature range of −269 to 400 °C and is commercially used in flexible printed circuits as insulating substrates. Therefore, it was chosen as the substrate material. Morphology, stoichiometry and electric properties of $Ba_xSr_{1-x}TiO_3$ films grown by hydrothermal synthesis on Kapton were investigated and discussed. Assessement of polar domains in the annealed hydrothermal $BaTiO_3$ films was conducted with the piezoresponse force microscopy (PFM).

Experimental Section

Commercial Kapton foils (Kapton 500HN) were supplied by Dupont. A Ti layer was deposited by RF magnetron sputtering (0.13 kW, 8 h) on a very thin Al buffer layer previously deposited by magnetron sputtering (0.04 kW, 20 min) on the Kapton to enhance the adhesion between the Ti layer and Kapton foil. The as-sputtered Ti layer composed of columnar grains had a flat upper-surface and a thickness around 8 μm as estimated by scanning electron microscopy (SEM) analysis.

$Ba_xSr_{1-x}TiO_3$ (x = 1, 0.9, 0.7, 05, 0.3, 0.1, and 0) films were prepared by a hydrothermal method. Kapton substrates with 1.5 cm × 1.5 cm size were immersed into 1 M alkaline solution of $Ba(OH)_2/Sr(OH)_2$. The alkaline solution was prepared with barium/strontium hydroxide octahydrate (99%, Merck) and boiled distilled water. Two or three pieces of substrates and 10 mL of the alkaline solution were put into one sealed autoclave vessel with 45 mL of capacity. The hydrothermal process was carried out at 120 °C for 1 h. Then, the products were washed with diluted acetic acid solution (17 wt %) and distilled water to remove the carbonates on the film surface. The films were dried at 60 °C in oven overnight. Some of the samples were annealed in flowing oxygen at 200 °C for 1 h.

Phase assembly of the films was analyzed by powder X-ray diffraction (XRD) using Cu Kα radiation (Rigaku Geigerflex D/max-c and X'Pert MPD Philips). Lattice parameters were calculated with the "Jade" program (version 8) via least-squares refinement based on the XRD patterns. Raman spectra were recorded in back-scattering geometry using a micro-Raman spectrometer (Labraw V 010) equipped with a He−Ne 632.8 nm laser. The morphology of the films was examined by SEM using an Hitachi S-4100 microscope equipped with an energy-dispersive spectroscopy (EDS) system for the stoichiometry evaluation. The films were coated with Au circular electrodes of 0.6 mm in diameter for electric measurements, while the unreacted Ti layer worked as bottom electrode. Capacitance density and dielectric loss of the thin films were evaluated with 0.1 V ac voltage using an LCR meter (HP 4284A). The leakage current data were collected with a Keithley 617 programmable electrometer. A modified commercial atomic force microscope (DI Nanoscope IIIa) was employed to characterize the local polarization of hydrothermal $BaTiO_3$ films. The scanning was performed in the contact mode using a conductive tip, and the maximum applied ac voltage was 5 V with a frequency of 50 kHz at zero bias field.

Results

Preliminary exploitation on the hydrothermal conditions to be used drew to the conclusion that long hydrothermal time resulted in the damage of Kapton substrate. The substrate became thinner and thinner after 3 h and completely broken into pieces after 6 h of soaking in 1 M $Ba(OH)_2$ solution at 120 °C. In addition, high hydrothermal temperature sometimes led to peeling off of the Ti−Al metal layers

(19) Balaraman, D.; Raj, P. M.; Wan, L.; Abothu, I. R.; Bhattacharya, S.; Dalmia, S.; Lance, M. J.; Swaminathan, M.; Sacks, M. D.; Tummala, R. R. *J. Electroceram.* **2004**, *13*, 95.
(20) Tan, C. K.; Goh, G. K. L.; Chi, D. Z.; Lu, A. C. W.; Lok, B. K. *J. Electroceram.* **2006**, *16*, 581.
(21) Roeder, R. K.; Slamovich, E. B. *J. Am. Ceram. Soc.* **1999**, *82*, 1665.
(22) Gersten, B. L.; Lencka, M. M.; Riman, R. E. *J. Am. Ceram. Soc.* **2004**, *87*, 2025.
(23) Xu, H.; Karadibhave, S.; Slamovich, E. B. *J. Am. Ceram. Soc.* **2007**, *90*, 2352.
(24) McCormick, M. A.; Roeder, R. K.; Slamovich, E. B. *J. Mater. Res.* **2001**, *16*, 1200.
(25) Zelonka, K.; Sayer, M.; Freundorfer, A. P.; Hadermann, J. *J. Mater. Sci.* **2006**, *41*, 3885.

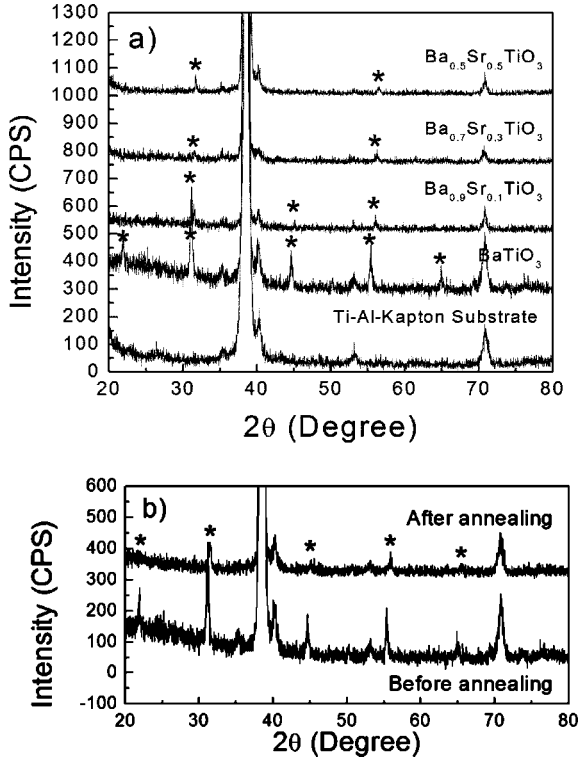

Figure 1. (a) XRD patterns of the hydrothermally synthesized $Ba_xSr_{1-x}TiO_3$ thin films on Ti−Al covered Kapton substrate before annealing; (b) XRD patterns of $BaTiO_3$ films before and after oxygen annealing. "*" indicates the peaks of perovskite phase.

from the substrate. The present films were then all prepared at 120 °C for 1 h.

Phase Assemblage and Film Morphology. XRD patterns of the as-synthesized films before oxygen annealing are shown in Figure 1a. Single $Ba_xSr_{1-x}TiO_3$ perovskite phase films free of carbonates were obtained on flexible Kapton substrates under the detection limit of the used equipment. With increasing strontium content, the peak intensity of the perovskite phase obviously decreased and the diffraction peaks shifted rightward to higher 2θ, indicating a reduction of the lattice parameter from 4.046 (±0.003) Å (for $BaTiO_3$) to 3.986 (±0.004) Å (for $Ba_{0.5}Sr_{0.5}TiO_3$) because of the smaller ionic radius of Sr^{2+}. For the composition $Ba_{0.3}Sr_{0.7}TiO_3$, the perovskite peaks were detectable only by glazing incidence XRD. The perovskite diffraction lines could not be observed neither under the normal nor glazing incidence XRD configurations for films with high strontium content ($Ba_{0.1}Sr_{0.9}TiO_3$ and $SrTiO_3$). Such unexpected results may be due to the following two possibilities: (i) absence of the perovskite phase, or (ii) too small film thickness to be detected with the used XRD equipment and measuring conditions. Raman spectroscopy was then used for further analysis. No well-defined Raman peaks were detected for $Ba_{0.1}Sr_{0.9}TiO_3$ and $SrTiO_3$ films, however broad signals in the range of 200−300, 500−600, and 700−800 cm^{-1}, consistent with the Raman characteristics of the perovskite structure of BST can be observed. The examination by microscopic analysis gave further information to clear up this question, as discussed below.

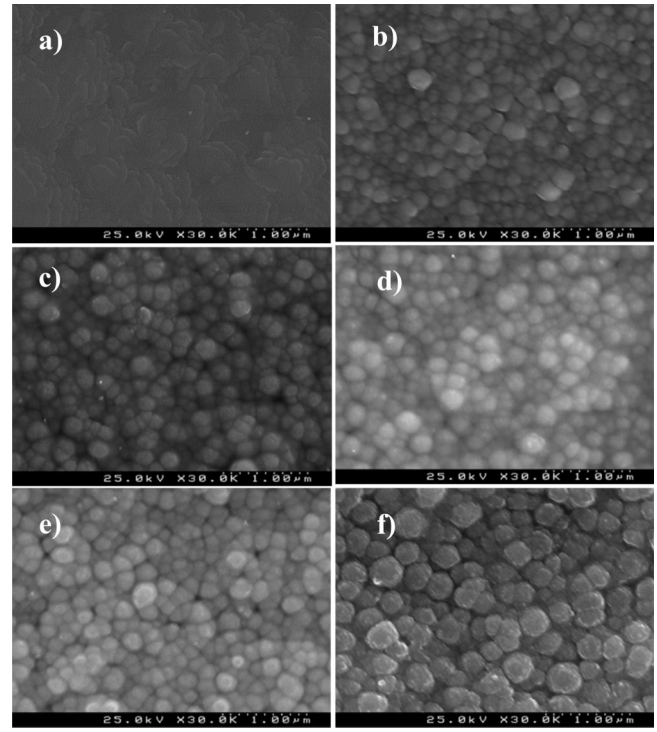

Figure 2. SEM surface micrographs of (a) the magnetron-sputtered Ti layer, (b) $BaTiO_3$, (c) $Ba_{0.7}Sr_{0.3}TiO_3$, (d) $Ba_{0.5}Sr_{0.5}TiO_3$, (e) $Ba_{0.3}Sr_{0.7}TiO_3$, and (f) $SrTiO_3$ films hydrothermally prepared at 120 °C for 1 h on flexible substrates before annealing.

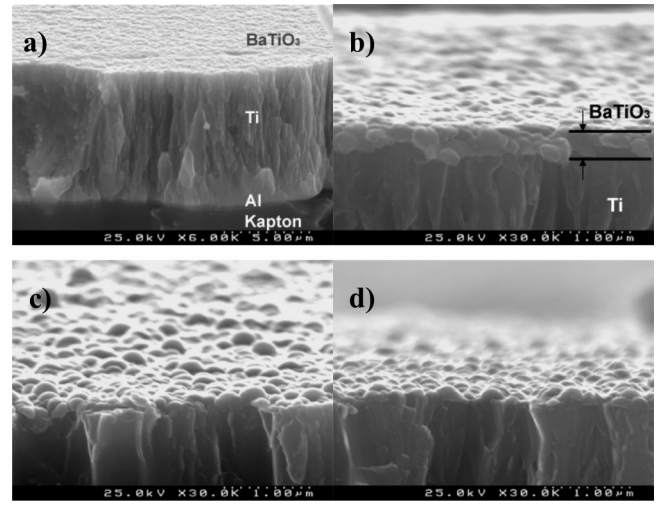

Figure 3. Cross-section SEM micrographs of the present samples. (a) $BaTiO_3$ films on Ti−Al covered Kapton substrate, (b) higher-magnification view of (a), (c) $Ba_{0.5}Sr_{0.5}TiO_3$, and (d) $SrTiO_3$ thin films before annealing.

A comparison between the patterns of $BaTiO_3$ films before and after oxygen annealing is shown in Figure 1b. The rightward shift of the diffraction peaks for annealed films clearly indicates the shrinkage of the unit cell during this post heat treatment process.

Surface and cross-section morphologies of the as-synthesized $Ba_xSr_{1-x}TiO_3$ films were inspected by SEM. Typical graphs are shown in Figure 2 and 3. In contrast to the flat surface of the magnetron-sputtered Ti layer, all the surfaces of hydrothermally prepared samples were covered with granular grains. $BaTiO_3$ films were composed of fine and densely compacted grains generally smaller than 200

nm except for a few coarse individual ones. With the substitution of strontium for barium, the grain size slightly increased. As for the other end member composition, $SrTiO_3$ ($x = 0$), the films were composed of coarse grains of 300−400 nm considerably larger than those of $BaTiO_3$ films. EDS results explicitly revealed the existence of Ba^{2+} and/or Sr^{2+} cations on the surface of all the $Ba_xSr_{1-x}TiO_3$ films with $x < 0.5$ for which the formation of the perovskite phase could not be confirmed by XRD. In addition, morphology similarity among the hydrothermally prepared $Ba_xSr_{1-x}TiO_3$ samples also supports the judgment of the successful formation of perovskite films for compositions of $x < 0.5$.

SEM cross-section graphs (Figure 3) are the definitive proof that perovskite thin films were deposited on the top surface of the Ti layer for all the studied compositions. $BaTiO_3$ films had a thickness of ca. 300 nm and were composed of layers of fine grains (Figure 3b). Thickness of the present $BaTiO_3$ films is analogous to those of the films prepared via a 24 h hydrothermal process.[19,20] For $SrTiO_3$ (Figure 3d), the films were indeed much thinner than those of $BaTiO_3$ and composed of only one layer of grains resulting in a rough surface, which should account for the absence of well-defined XRD peaks of the perovskite phase. Thin films of intermediate compositions ($0 < x < 1$) possessed morphologies in between those of the two-end compositions, as depicted in the SEM cross-section micrograph of $Ba_{0.5}Sr_{0.5}TiO_3$ films in Figure 3c. The observed decreasing film thickness is consistent with the weakening of XRD signals from Ba-rich compositions to Sr-rich compositions. The variation of the film morphology reflects a dependence of the hydrothermal reaction kinetics on the composition of the solid solution.

Deviation of Ba/Sr Ratio. Stoichiometry control is an important aspect in hydrothermal synthesis. EDS spectra of the hydrothermally synthesized films are shown in Figure 4a. The analysis exhibited a deviation of Ba content from the nominal x in $Ba_xSr_{1-x}TiO_3$ (Figure 4b), especially in Ba-rich composition region. For instance, although the concentration ratio between $Ba(OH)_2$ and $Sr(OH)_2$ in the initial solution was 7:3 for the nominal $Ba_{0.7}Sr_{0.3}TiO_3$, the measured content of barium and strontium almost equaled each other for the produced films. The deviation became weakened for Sr-rich compositions. Similar effect related with the "preferred incorporation" of strontium into the perovskite lattice of $Ba_xSr_{1-x}TiO_3$ solid solution was reported in the literature as well and justified by lower formation energy of $SrTiO_3$.[21,23,24]

Electrical Characterization. The capacitance density and dielectric loss ($\tan\delta$) under weak ac field were measured at room temperature for $Ba_xSr_{1-x}TiO_3$ films on Kapton before and after oxygen annealing. The data as function of frequency for $BaTiO_3$, $Ba_{0.5}Sr_{0.5}TiO_3$, and $SrTiO_3$ films are shown in Figure 5. The as-synthesized films exhibited high capacitance density above 1 μF/cm^2 as well as high dielectric loss. Both the capacitance density and tan δ were lowered after oxygen annealing. At 100 kHz, a capacitance density of 0.44 μF/cm^2 and tan δ of 0.04 were attained in annealed $BaTiO_3$ thin films with the corresponding dielectric constant being around 150. Annealed $Ba_{0.5}Sr_{0.5}TiO_3$ and $SrTiO_3$ films had even higher capacitance density of 0.64 and 0.76 μF/cm^2, respectively, at 100 kHz, most probably because of their smaller thickness as described in the previous session. Considering that the film thickness of $Ba_{0.5}Sr_{0.5}TiO_3$ was between 200−300 nm, and $SrTiO_3$ was between 100−200 nm, the dielectric constant of $Ba_{0.5}Sr_{0.5}TiO_3$ and $SrTiO_3$ thin films was estimated in the range of 145−217 and 86−172, respectively. Besides, the strong frequency dependence of capacitance density was also weakened with the oxygen annealing. A comparison about the dielectric properties of hydrothermally prepared $BaTiO_3$ films reported in this work and in the literature is illustrated in Table 1. The present films prepared via 1 h hydrothermal process are comparable and competitive when compared with those derived from long-time hydrothermal reactions.

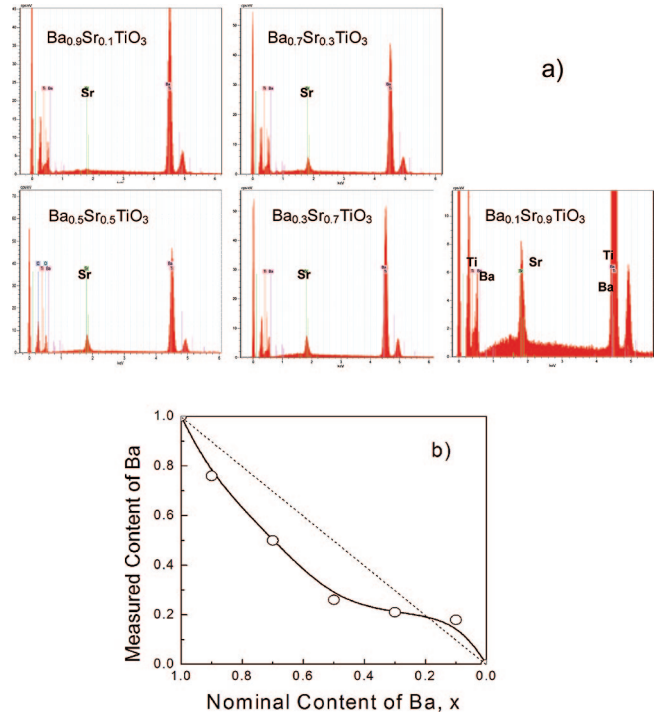

Figure 4. (a) EDS spectra of the hydrothermal $Ba_xSr_{1-x}TiO_3$ thin films. Spectrum of $Ba_{0.1}Sr_{0.9}TiO_3$ is displayed with a larger scale showing the details of Sr, Ba, and Ti signals. (b) Deviation of Ba content measured by EDS from the nominal content x.

Typical dc leakage current characteristics of annealed $BaTiO_3$, $Ba_{0.5}Sr_{0.5}TiO_3$ and $SrTiO_3$ films as well as the as-synthesized $BaTiO_3$ films are given in Figure 6. Under relatively low voltage (<1 V), the leakage current of annealed $BaTiO_3$ films was of the order of 1×10^{-8} A/cm^2. An accelerated increase began around 1 V (corresponding to an electric field of ~33 kV/cm) suggesting a transition from ohmic conduction to field induced electron emission region. Here, oxygen vacancies and cation vacancies coupled with remnant hydroxyl group are believed to be the major cause of the leakage current in the ohmic conduction region. $Ba_{0.5}Sr_{0.5}TiO_3$ and $SrTiO_3$ films exhibited a quick increase of leakage current with applied dc voltage, which should be attributed to the one-layered microstructure where short circuit could easily appear. The as-synthesized $BaTiO_3$ films

(26) Wei, Z.; Noda, M.; Okuyama, M. *Integr. Ferroelectr.* **2003**, *52*, 111.

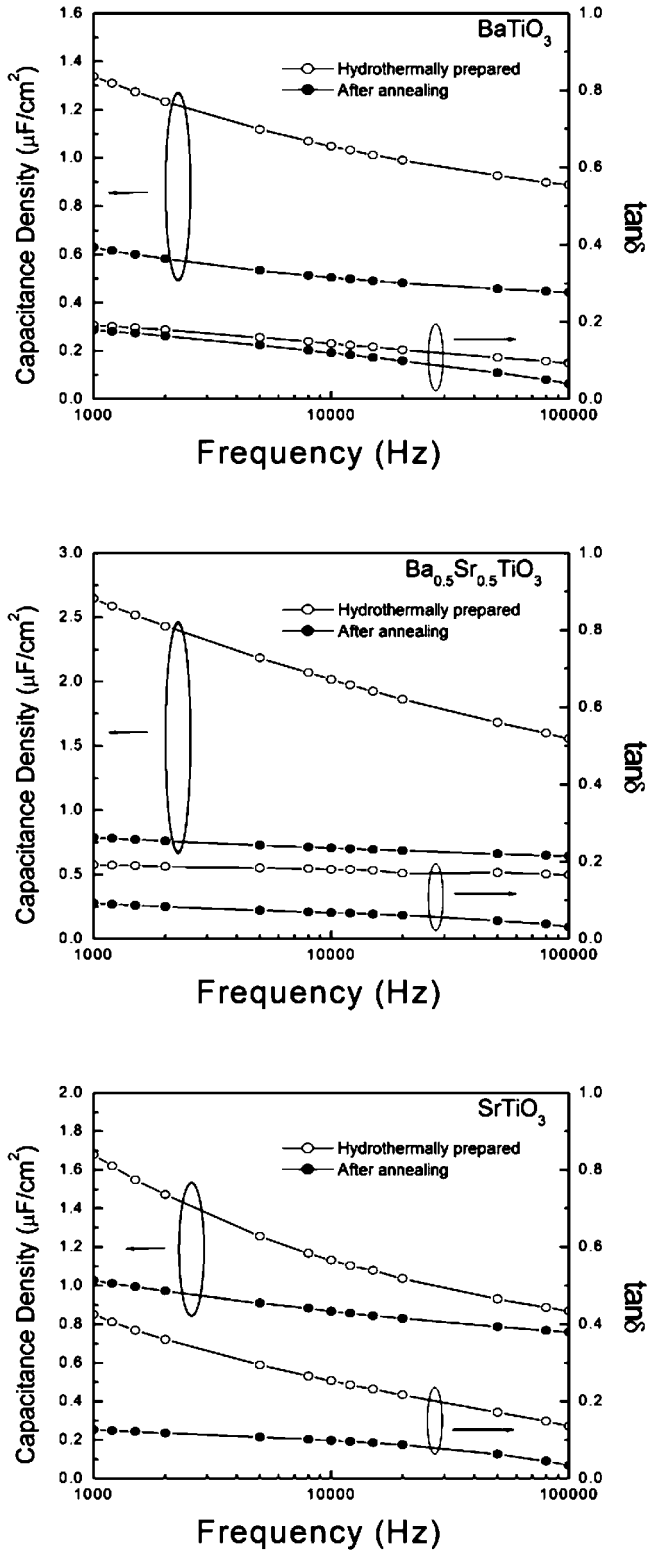

Figure 5. Capacitance density and tanδ as function of frequency for $Ba_xSr_{1-x}TiO_3$ thin films on Kapton before and after 200 °C annealing in flowing oxygen.

showed much higher leakage current density compared with annealed films and broke down when voltage was above 0.5V.

In accordance with the dielectric response just presented, the polarization versus electric field ($P-E$) relation of the current films had the characteristics of lossy dielectrics, hiding the polarization switching behavior. So another technique had to be employed to check whether these hydrothermal films were in the polar phase state. PFM is an effective technique to observe ferroelectric domain structures at the nanoscale.[27] As far as the authors know, there are no reports concerning PFM studies on hydrothermally prepared $BaTiO_3$ thin films yet. Figure 7 shows two- and three-dimensional topography and piezo-response images obtained on annealed $BaTiO_3$ films. The existence of polar domains in hydrothermal $BaTiO_3$ films was proved by the distinct piezo-response signal contrast (Figure 7c). Here, the direction of the out-of-plane component of polarization was distinguished by the phase between the driving voltage and measured displacement through a lock-in amplifier. In principle, piezo-response signal (Z[V]) sensed by PFM is proportional to the applied voltage V_{ac} and the effective piezoelectric coefficient [$(d_{33})_{eff}$] of the material: (Z[V]) $\propto$ $(d_{33})_{eff}V_{ac}\cos\varphi$, where φ stands for the phase shift between the driving voltage and the measured ac vibration ($\varphi = 180°$ for positive domains and $\varphi = 0$ for negative domains). Therefore, domains with opposite polarities have different contrast in the piezo-response image. The observed bright and dark regions in Figure 7c represent domains orienting toward the top surface and bottom substrate, respectively. Figure 7d gives the cross-sectional profile analysis corresponding to the line drawn in Figure 7b and 7c across three consecutive adjacent grains. A poly domain structure was found in the left grain, whereas the other two had single domains but with opposite polarity.

Discussion

Hydrothermal synthesis of perovskite compounds is a rather complicated process, depending on experimental parameters as temperature, reaction time, pH value, reactants and their concentrations.[28−31] Formation of the current $Ba_xSr_{1-x}TiO_3$ thin films can be described by the following three steps: (i) dissolution of Ti from substrate into solution to form soluble species; (ii) nucleation of $Ba_xSr_{1-x}TiO_3$ on the upper surface of substrate under supersaturation conditions; (iii) grain growth to cover the substrate surface into an integral film.

In this work, a decrease in the film thickness from Ba-rich to Sr-rich compositions accompanied by an increase of the grain size clearly indicates a composition dependence of the film morphology. For the same film area, the relatively larger number of grains of $BaTiO_3$ films suggests a higher primary nucleation rate than that of $SrTiO_3$. The primary nucleation rate is related to temperature, reactant concentration, diffusion coefficient of solute, Gibbs free energy barrier for nucleation, etc.[31−33] The smaller hydrated radius of Ba^{2+} than Sr^{2+} favors its diffusion in the solution, and in turn, favors the nucleation. Another plausible reason for the high nucleation rate of $BaTiO_3$ is the stronger alkalinity of

(27) Gruverman, A.; Kholkin, A. *Rep. Prog. Phys.* **2006**, *69*, 2443.
(28) Lencka, M. M.; Riman, R. E. *Chem. Mater.* **1993**, *5*, 61.
(29) Lencka, M. M.; Riman, R. E. *Ferroelectrics* **1994**, *151*, 159.
(30) Lencka, M. M.; Riman, R. E. *Chem. Mater.* **1995**, *7*, 18.
(31) Testino, A.; Buscaglia, V.; Buscaglia, M. T.; Viviani, M.; Nanni, P. *Chem. Mater.* **2005**, *17*, 5346.
(32) Kutty, T. R. N.; Padmini, P. *Mater. Chem. Phys.* **1995**, *39*, 200.
(33) Dirksen, J. A.; Ring, T. A. *Chem. Eng. Sci.* **1991**, *46*, 2389.

Table 1. Synthesis Conditions and Dielectric Properties of Hydrothermal $BaTiO_3$ Thin Films Prepared in This Work and Some Other Reports; Films Prepared by Hydrothermal−Electrochemical Method Are Not Included

substrate	synthesis temperature (°C)	reaction time	dielectric constant	tan δ	measuring frequency (Hz)	ref.
Kapton	120	1 h	140	0.04	100 k	Present work[a]
PCB[b]	95	24 h	370	0.06	100 k	19[a]
PCB[c]	80	24 h	~350	~0.1	100 k	20[a]
Pt-coated class	90	4 h	45	0.026	not indicated	11[a]
Ti foil	240	1−4 weeks	400−500	<0.05	1 k	14
$Pt/Ti/SiO_2/Si$	200	8 h	20	<0.25	not indicated	26

[a] Indicates samples after oxygen annealing or plasma treatment. [b] FR4, typical rigid PCB substrate. [c] Copper cladded BT 832 epoxy laminate.

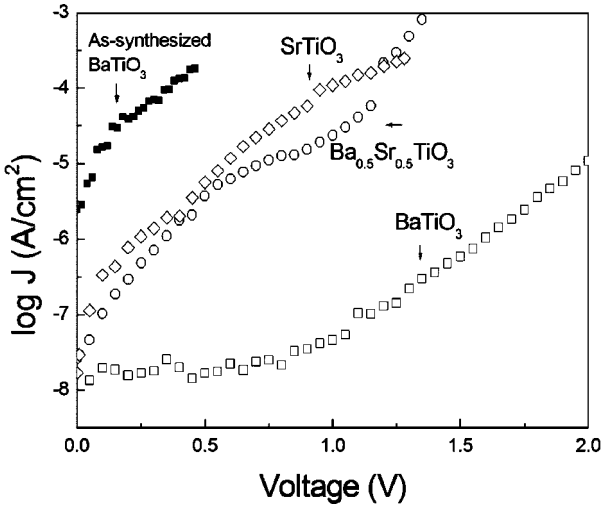

Figure 6. $J-V$ behaviors of $Ba_xSr_{1-x}TiO_3$ thin films on Kapton after annealing treatment. Curve of as-synthesized $BaTiO_3$ films is also shown as a comparison.

$Ba(OH)_2$ than $Sr(OH)_2$ leading to an easier dissolution of titanium from the substrate surface into the solution in the form of hydrate as $[Ti(OH)_4]$ or $[Ti(OH)_6]^{2-}$. High concentration of soluble titanium species certainly promotes the formation of $BaTiO_3$ embryos. In addition, the thicker $BaTiO_3$ films indicate a higher reaction rate under the present hydrothermal condition than that of $SrTiO_3$. This is entirely consistent with the results of the work of Xu et al. about the composition effects on the reaction kinetics of barium strontium titanate powders, where the perovskite phase formation increased monotonically with the Ba content in barium strontium titanate.[23] However, in Xu's work, a much faster particle growth of $BaTiO_3$ over $SrTiO_3$ was reported, which seems to differ from the present results. Space restrictions for the grain/particle growth in the case of thin films because of the limited substrate area is suggested as the reason for the observed difference. The high embryo density of $BaTiO_3$ caused a severe growth competition among neighboring embryos and finally led to a frustration of further grain/particle expansion. In contrast, the relatively few embryos of $SrTiO_3$ at the first stage of hydrothermal process allowed more space for grains/particles to grow. In the case of powders, particles can grow freely either by secondary nucleation or aggregation because there is no space restriction.

Apparently, the "preferred incorporation" of strontium into the perovskite lattice in hydrothermally prepared barium strontium titanates should not be attributed to kinetic aspects. In the thermodynamic modeling work of Lencka et al., phase stability diagrams were proposed for hydrothermal Ba−Ti and Sr−Ti systems based on both standard-state thermodynamic data and activity coefficient model.[28−30] The comparison between the diagrams revealed that a much lower concentration of strontium is required for the formation of the perovskite phase than that of barium under the same conditions.[30] Combining the discussion in the previous paragraphs, it appears that the formation of $SrTiO_3$ is thermodynamically favorable but $BaTiO_3$ has faster kinetics once the thermodynamic condition is satisfied. Further studies are needed to give a clear interpretation.

The dielectric properties of the fabricated thin films were greatly influenced by the microstructures. Dense $BaTiO_3$ films constructed by layers of fine grains had a low leakage current. The $Ba_{0.5}Sr_{0.5}TiO_3$ and $SrTiO_3$ thin films with less dense microstructures and incipient degree of crystallinity due to low reaction rate caused enhanced charge transportation, which is responsible for their different $J-V$ behaviors from that of $BaTiO_3$.

It is known that defects are unavoidable in hydrothermal synthesis of $Ba_xSr_{1-x}TiO_3$ materials. In some cases, phase transitions may be inhibited due to the suppression of the structure deformation by defects.[34] Measurements of $P-E$ relation for hydrothermally synthesized $BaTiO_3$ films also suffer from the interference of slow charge relaxations. To mitigate these consequences, postannealing treatments are usually conducted. The effects of postannealing in the fabrication of hydrothermal thin films are widely accepted as the removal of hydroxyl groups residing both in the perovskite lattice and on the surface of the films.[11,20,35] The observed decrease of capacitance density after oxygen annealing (Figure 5) resulted from the exclusion of the polarization contribution from the hydroxyl groups. At the same time, the removal of lattice hydroxyl groups is supposed to generate water molecules and leave oxygen vacancies that should be compensated by the oxygen atmosphere thermal treatment. According to the XRD analysis on the films before and after annealing (Figure 1b), there was an obvious decrease in the lattice parameter from 4.046 (±0.003) Å to 4.010 (±0.006) Å, strongly implying that low annealing temperature of 200 °C, which is compatible with the currently used polymeric flexible substrate, can be effective to remove the hydroxyl group residues in the perovskite lattice. Besides, the large decrease of the leakage current density after oxygen annealing observed for $BaTiO_3$ films (Figure 6) is another evidence for the removal of lattice defects.

(34) Shi, E. W.; Xia, C. T.; Zhong, W. Z.; Wang, B. G.; Feng, C. D. *J. Am. Ceram. Soc.* **1997**, *80*, 1567.
(35) Chien, A. T.; Xu, X.; Kim, J. H.; Sachleben, J.; Speck, J. S.; Lange, F. F. *J. Mater. Res.* **1999**, *14*, 3330.

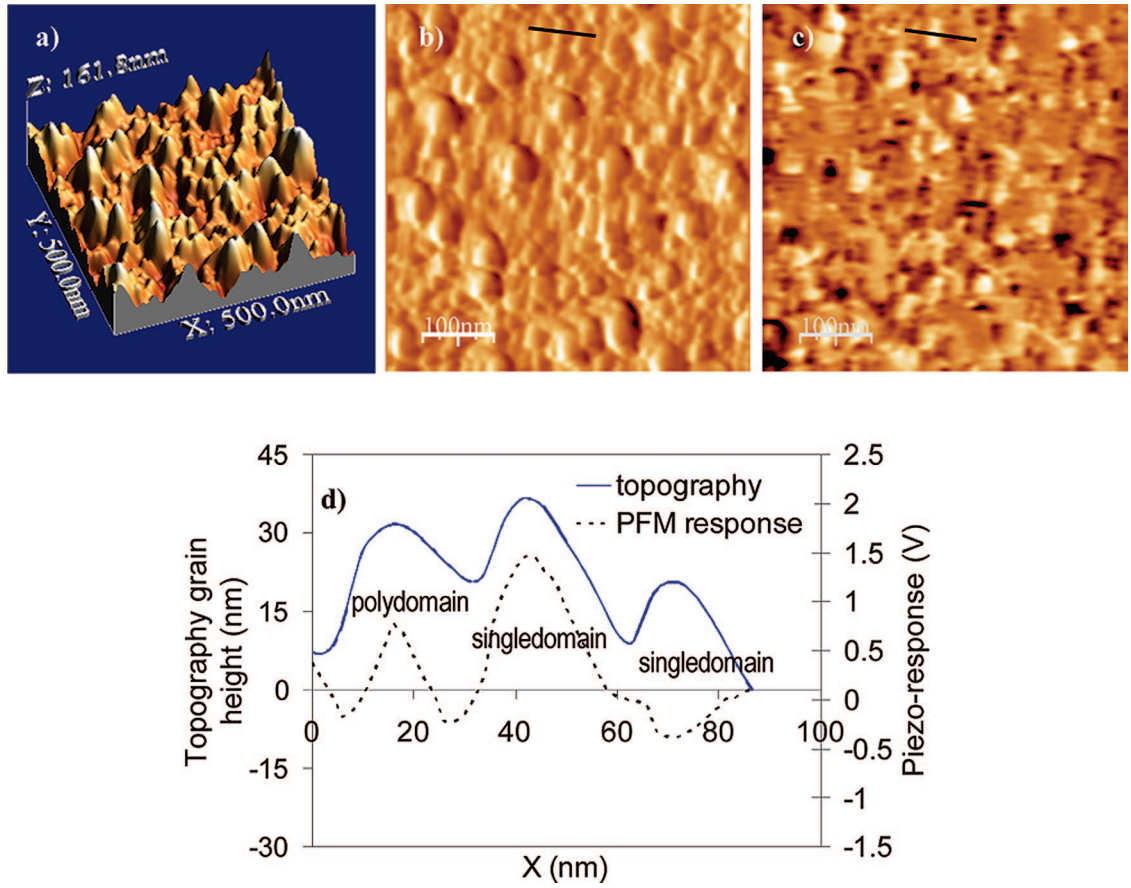

Figure 7. (a) Three dimensional and (b) two-dimensional topographic and (c) piezo-response images of annealed hydrothermal $BaTiO_3$ thin films on Kapton. (d) Corresponding cross-section line profile analysis on both (b) topographic and (c) piezo-response images.

XRD patterns of the present films were indexed to a pseudocubic structure because there was no discernible splitting of the related peaks. However, this absence should not be considered as the ultimate proof of the nonexistence of a tetragonal structure or a degree of tetragonality in the $BaTiO_3$ films. It is well-known that the XRD peak splitting related to the tetragonal distortion of $BaTiO_3$ becomes weak as the grain size decreases.[36] In general, nanograined $BaTiO_3$, as the one of this work, is considered as mixture of cubic and tetragonal phases. Distortion of cubic lattice into a polar structure in the $BaTiO_3$ films was evident via the observation of the distinct contrast in PFM image. Domain splitting in grains occurs under high mechanical tension to achieve a reduction of total stress. The observation of poly domains implies a stressed state of the present hydrothermal films.

Summary

$Ba_xSr_{1-x}TiO_3$ thin films were grown via a polymer-compatible hydrothermal process on flexible Kapton substrate. Although the reaction time was limited to only one hour, dense $Ba_xSr_{1-x}TiO_3$ ($x \geq 0.5$) thin films were attained, whereas higher strontium content led to an "incipient" degree of crystallinity of the films. $BaTiO_3$ films exhibited a higher nucleation rate than $SrTiO_3$ under the same hydrothermal conditions. The composition stoichiometry analysis suggested a preference for the incorporation of strontium into the perovskite lattice. As-synthesized films showed high capacitance density and tanδ values which were both decreased to acceptable ones by annealing in oxygen (0.44 μF/cm^2 and tanδ of 0.04 for $BaTiO_3$ at 100 kHz). Polar domains in the hydrothermally synthesized $BaTiO_3$ films were clearly distinguished by PFM analysis. All the experimental processes designed in this work are compatible with the use of polymers, making this route possible to be extended to the synthesis of other materials and on other polymeric flexible substrates for new generation of electronic packaging.

Acknowledgment. The authors are thankful to Dr. D. L. Sun for Raman experiments, Dr. J. S. Liu for the assistance of PFM characterization, and all the technicians involved. The authors acknowledge financial support from FCT under Grant SFRH/BPD/26711/2006, FEDER, and the European Network of Excellence FAME under Contract FP6-500159-1.

CM802845S

(36) (a) Petkov, V.; Buscaglia, V.; Buscaglia, M. T.; Zhao, Z.; Ren, Y. *Phys. Rev. B* **2008**, *78*, 054107. (b) Buscaglia, V.; Buscaglia, M. T.; Viviani, M.; Mitoseriu, L.; Nanni, P.; Trefiletti, V.; Piaggio, P.; Gregora, I.; Ostapchuk, T.; Pokorný, J.; Petzelt, J. *J. Eur. Ceram. Soc.* **2006**, *26*, 2889.